

**QUICK SEARCH:** [\[advanced\]](#)

Go  Author:  Keyword(s):

Year:  Vol:  Page:

Published online before print June 26, 2006,  
10.1148/radiol.2402050972

(Radiology 2006;240:522-528.)

## Special Report

# Virtual Autopsy: Preliminary Experience in High-Velocity Gunshot Wound Victims<sup>1</sup>

Angela D. Levy, LTC, MC, USA, Robert M. Abbott, Lt Col, USAFR, MC, Craig T. Mallak, CDR, MC, USN, John M. Getz, BS, H. Theodore Harcke, COL, MC, ARNG, Howard R. Champion, MD and Lisa A. Pearse, MAJ, MC, USA

<sup>1</sup> From the Department of Radiologic Pathology, Armed Forces Institute of Pathology, Alaska and Fern Streets NW, Washington, DC 20306-6000 (A.D.L., R.M.A., H.T.H.); Office of the Armed Forces Medical Examiner, Armed Forces Institute of Pathology, Rockville, Md (C.T.M., J.M.G., L.P.); Department of Radiology, University of Maryland School of Medicine, Baltimore, Md (R.M.A.); Departments of Radiology and Nuclear Medicine (A.D.L., R.M.A., H.T.H.) and Surgery and Military and Emergency Medicine (H.R.C.), Uniformed Services University of the Health Sciences, Bethesda, Md. Received June 13, 2005; revision requested August 2; revision received August 3; accepted September 6; final version accepted October 4. Supported by a grant from the Defense Advanced Research Projects Agency. Address correspondence to A.D.L. (e-mail: [levya@afip.osd.mil](mailto:levya@afip.osd.mil)).

### This Article

- ▶ [Abstract](#) **FREE**
- ▶ [Figures Only](#)
- ▶ [Full Text \(PDF\)](#)
- ▶ **All Versions of this Article:**  
[2402050972v1](#)  
**240/2/522 *most recent***
- ▶ [Submit a response](#)
- ▶ [Alert me when this article is cited](#)
- ▶ [Alert me when eLetters are posted](#)
- ▶ [Alert me if a correction is posted](#)

### Services

- ▶ [Email this article to a friend](#)
- ▶ [Similar articles in this journal](#)
- ▶ [Similar articles in PubMed](#)
- ▶ [Alert me to new issues of the journal](#)
- ▶ [Download to citation manager](#)
- ▶ [© Get Permissions](#)

### Citing Articles

- ▶ [Citing Articles via HighWire](#)
- ▶ [Citing Articles via Google Scholar](#)

### Google Scholar

- ▶ [Articles by Levy, A. D.](#)
- ▶ [Articles by Pearse, L. A.](#)
- ▶ [Search for Related Content](#)

### PubMed

- ▶ [PubMed Citation](#)
- ▶ [Articles by Levy, A. D.](#)
- ▶ [Articles by Pearse, L. A.](#)

▲ <a href="#">TOP</a>
▪ <a href="#">ABSTRACT</a>
▼ <a href="#">INTRODUCTION</a>
▼ <a href="#">MATERIALS AND METHODS</a>
▼ <a href="#">RESULTS</a>
▼ <a href="#">DISCUSSION</a>
▼ <a href="#">ADVANCES IN KNOWLEDGE</a>
▼ <a href="#">References</a>

## ▶ ABSTRACT

**Purpose:** To retrospectively assess virtual autopsy performed with multidetector computed tomography (CT) for the forensic evaluation of gunshot wound victims.

**Materials and Methods:** The institutional review board approved this HIPAA-compliant study and did not require informed consent of the next of kin. Thirteen consecutive male gunshot wound victims (mean age, 27 years) were scanned with 16-section multidetector CT prior to routine autopsy. Retrospectively, the total-body nonenhanced scans were interpreted at a three-dimensional workstation by radiologists blinded to autopsy findings. Images were evaluated for lethal wound, number and location of wound tracks, injured structures, and metal fragment location. After image review, autopsy reports and photographs were compared with the images and interpretations to validate the multidetector CT determinations.

**Results:** Multidetector CT aided in correct identification of all lethal wounds, and metallic fragment location was always precise. In four cases, multidetector CT aided in accurate assessment of organ injuries and lethal wounds but led to underestimation of the number of wounds if comingling paths occurred. In two cases of a chest wound, multidetector CT aided in accurate assessment of the chest as having the lethal wound but failed to help identify specific sites of hemorrhage. In two cases of craniofacial injury, the path of the wound was not clear. Autopsy revealed a total of 78 wound tracks (mean, 6; range, 1–24). Ten (13%) wound tracks were not identified at multidetector CT (six upper extremity wounds and four thigh wounds). In two cases, findings missed at autopsy (fracture of the cervical spine, bullet fragments in the posterior area of the neck) were identified at multidetector CT.

**Conclusion:** Multidetector CT can aid prediction of lethal wounds and location of metallic fragments.

## ▶ INTRODUCTION

The role of full-body radiography in autopsy and forensic investigation is well established and routinely applied to document fractures, injury patterns, occult injuries, and foreign body and metallic fragment localization and to aid in the identification of human remains when conventional methods such as fingerprinting or DNA analysis are not available or cannot be used (1–3). The role of radiology in autopsy has been expanded to include multidetector computed tomography (CT) and magnetic resonance (MR) imaging. Thali et al (4) apply the term *virtual autopsy* or *virtopsy* to the technique of postmortem imaging with multidetector CT and/or MR imaging.

▲[TOP](#)  
▲[ABSTRACT](#)  
- [INTRODUCTION](#)  
▼[MATERIALS AND METHODS](#)  
▼[RESULTS](#)  
▼[DISCUSSION](#)  
▼[ADVANCES IN KNOWLEDGE](#)  
▼[References](#)

Radiography is invaluable in the forensic investigation of gunshot wounds and is universally used to locate the bullet, identify the type of ammunition and weapon used, document the path of the bullet, and to assist in the retrieval of the bullet (5). The pattern of metal fragment distribution along the path of the bullet is an indication of the type of ammunition used. Moreover, recovery of the bullet jacket is critical in forensic investigation because the jacket contains unique rifling characteristics that enable ballistics experts to identify the weapon from which the bullet was fired. Bullet jackets are typically made of copper or copper alloys and are easily distinguished from the lead core of the bullet on radiographs (5). Penetrators, small conical pieces of metal located in the tip of the bullet, are designed to stiffen the bullet to penetrate the target. Penetrators may fragment from the rest of the bullet and have a characteristic appearance at radiography and when recovered at autopsy. Thali et al (6) have shown that virtual autopsy in gunshot wound victims is useful to localize the bullet in three dimensions, document the bullet path, visualize fracture patterns associated with gunshot wounds, and evaluate internal organ injury prior to autopsy. We undertook our study to retrospectively assess virtual autopsy performed with multidetector CT for the forensic evaluation of gunshot wound victims.

▲[TOP](#)  
▲[ABSTRACT](#)  
▲[INTRODUCTION](#)  
- [MATERIALS AND METHODS](#)  
▼[RESULTS](#)  
▼[DISCUSSION](#)  
▼[ADVANCES IN KNOWLEDGE](#)  
▼[References](#)

## ▶ **MATERIALS AND METHODS**

### **Study Group**

The study population included 13 consecutive male gunshot wound victims (age range, 19–49 years; mean age, 27 years) who underwent routine autopsy in December 2004 at a single

institution. All of the subjects sustained lethal injuries from high-velocity 7.62-mm ammunition that is used in AK-47 assault weapons and some machine guns. This Health Insurance Portability and Accountability Act-compliant study was performed with institutional review board approval; the board did not require informed consent from next of kin.

### **CT and Autopsy Technique**

All subjects were imaged prior to autopsy with total-body multidetector CT (LightSpeed 16; GE Medical Systems, Milwaukee, Wis) within 2–5 days (mean, 3.5 days) of death. Two series of images were obtained in each subject. Images in series 1 were obtained from the skull vertex to the most distal point allowable with table travel (distal femur or proximal tibia and fibula). Images in series 2 were obtained from the superior aspect of the acetabulum to the toes. All subjects were scanned with 16 detector rows and 5-mm section thickness (16 x 5 mm), pitch of 1.75:1, rotation speed of 0.5 second, and table speed of 35 mm per rotation. No contrast material was administered. Images were retrospectively reconstructed at the CT console to a section thickness of 1.25 mm prior to being sent to a workstation (Advantage, software version 4.2; GE Medical Systems).

Four board-certified forensic pathologists with 8–19 years of experience who were from the Office of the Armed Forces Medical Examiner, Armed Forces Institute of Pathology, Rockville, Md, performed all autopsies. Each autopsy included a digital skeletal survey (drrMulti-system; Swissray International, Elizabeth, NJ) and digital photography. Digital photographs were obtained of the external appearance of the body, gunshot entry and exit wounds, probed gunshot wound tracks, internal organ injury, and recovered metal fragments. Complete dissection of the intracranial contents, oral cavity, neck, chest, abdomen, and pelvis was performed in each case. All internal organs were examined. All metallic fragments associated with major wounds were documented and removed for evidence collection.

### **Image Interpretation**

Retrospectively, two radiologists (A.D.L., R.M.A.), each with 12 years of experience, interpreted the total-body scans. The radiologists were blinded to the final autopsy results. Final image interpretation was reached with consensus. Images were interpreted at the workstation by using two-dimensional transverse, coronal, oblique, and sagittal data sets, as well as three-dimensional volume-rendered images.

Images were evaluated to determine the lethal gunshot wound and the number and location of all gunshot wound tracks. Wound tracks were identified by the presence of gas, hemorrhage, bone, or metal in a linear distribution through soft tissues and organs. Once a track was identified, it was visually connected to possible entry and exit defects in the skin. The directionality of bone and metal fragments and the beveling of bone were used to determine the bullet trajectory. Entry wounds were also suggested when there were bone and/or metal fragments driven in beyond the skin or bone defect. The location of all metal fragments was noted.

All soft tissue, organ, and skeletal injuries were documented. The CT scan was read as positive for organ injury if there was gas, fluid, or loss of integrity of the normal appearance of the organ. Vascular injury was defined as disruption of the vessel or cardiac chamber wall. The finding of gas alone within vascular spaces was excluded as a positive finding because intravascular gas is a

normal decompositional finding in the postmortem state. The characteristic of hemorrhage (high attenuation or fluid attenuation) was noted when present in the soft tissues, brain, lung, and liver. The presence of hemorrhage and/or gas in the trachea, mediastinum, bronchi, pleural space, pericardial space, and peritoneum also was documented. Gastrointestinal injury was defined as focal thickening or discontinuity of the bowel wall. Mesenteric injury was defined as infiltration or thickening of the mesentery.

### **Autopsy Comparison**

After image review, two- and three-dimensional data sets were reviewed and compared with the final autopsy reports and photographs by three radiologists (A.D.L., R.M.A., and H.T.H., with 12–30 years of experience), one forensic pathologist (C.T.M., with 14 years of experience), and one trauma surgeon (H.R.C., with 33 years of experience). The lethal gunshot wound, location of wound tracks, and sites of organ injury were compared with the CT findings. The number, location, and characteristics (copper jacket, lead core, or steel penetrator) of recovered metallic fragments were compared with the fragments identified at CT. All gunshot wounds were classified as high-velocity wounds because the following features of high-velocity gunshot wounds were present at autopsy: passage of the bullet through the body, temporary cavities along the path of the bullet, and fragmentation of the bullet along its path.

[▲TOP](#)  
[▲ABSTRACT](#)  
[▲INTRODUCTION](#)  
[▲MATERIALS AND METHODS](#)  
• RESULTS  
[▼DISCUSSION](#)  
[▼ADVANCES IN KNOWLEDGE](#)  
[▼References](#)



## **RESULTS**

### **Lethal Gunshot Wounds and Track Location**

Multidetector CT aided in correct identification of the lethal wounds (six head, three chest, and four head and chest wounds) in all subjects. In 13 subjects, there were a total of 78 wound tracks identified at autopsy. At autopsy, the number of wound tracks per subject ranged from one to 24 (mean, six) and were located in the head ( $n = 14$ ), face and neck ( $n = 10$ ), chest ( $n = 21$ ), abdomen ( $n = 3$ ), buttock ( $n = 2$ ), right shoulder ( $n = 1$ ), left shoulder ( $n = 2$ ), left axilla ( $n = 1$ ), right upper extremity ( $n = 5$ ), left upper extremity ( $n = 5$ ), right lower extremity ( $n = 8$ ), left lower extremity ( $n = 3$ ), and left hand and wrist ( $n = 3$ ). Multidetector CT aided in the correct prediction of 68 (87%) of the gunshot wound tracks. The 10 (13%) tracks that were not identified prospectively at multidetector CT were located in the upper extremity ( $n = 6$ ) and thigh ( $n = 4$ ). Five of the missed upper extremity tracks were located in the proximal forearm or were proximal to the elbow such that they were excluded from the scanning field of view because of a bend in

the elbow. One upper extremity track that was not identified prospectively was in the wrist. The four thigh wounds that were missed were missed because of perceptive errors. In each case, a small metal fragment was initially identified; however, the wound track was subtle and overlooked.

The directions of the gunshot wound paths were accurately predicted in nine (69%) victims ([Fig 1](#)). In the four cases in which prediction was not correct, the subjects had multiple gunshot wounds with intersecting and comingling paths. In two cases, the subjects had multiple gunshot wounds to the head with intersecting paths that resulted in innumerable calvarial and skull base fractures; therefore, the standard features of bone beveling, the pattern of metal deposition, or the bone fragment displacement used to determine gunshot track directionality could not be applied. In the third case, the subject sustained two gunshot wounds to the abdomen from opposite directions with intersecting paths. Finally, the subject of the fourth case sustained nine gunshot wounds to the posterior chest. In this case, the number of gunshot wounds and path directionality could not be predicted prospectively by using multidetector CT nor convincingly ascertained at autopsy.



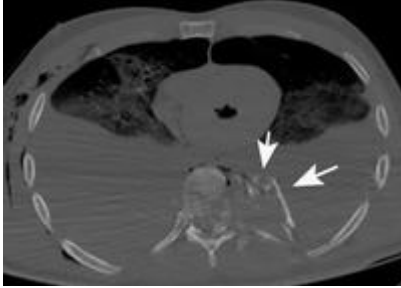
**View larger version (113K):**

[\[in this window\]](#)

[\[in a new window\]](#)

[\[Download PPT slide\]](#)

**Figure 1a:** Lethal gunshot wound to the chest. **(a, b)** Transverse nonenhanced CT image shows the entry wound as an irregular linear soft-tissue defect in the right anterior chest (arrow in **a**) with associated subcutaneous gas. The bullet passed from right to left through the midthoracic vertebral bodies. Bone fragments are present to the left of the vertebral body (arrows in **b**). The displacement of bone fragments leftward indicates the direction of the bullet path. There are retropulsed fragments within the spinal canal. The bilateral hemothoraces resulted from aortic transection, which was not evident at CT. The aorta is collapsed and not visualized. **(c)** Surface-rendered image of CT data shows the entry wound lateral to the right nipple (arrow). **(d)** Correlative photograph at autopsy shows the entrance wound. **(e)** Photograph at autopsy shows bone fragments protruding from the midthoracic spine (arrows), angled in the direction of the path of the bullet.



**View larger version (81K):**

[\[in this window\]](#)

[\[in a new window\]](#)

[\[Download PPT slide\]](#)

**Figure 1b:** Lethal gunshot wound to the chest. **(a, b)** Transverse nonenhanced CT image shows the entry wound as an irregular linear soft-tissue defect in the right anterior chest (arrow in **a**) with associated subcutaneous gas. The bullet passed from right to left through the midthoracic vertebral bodies. Bone fragments are present to the left of the vertebral body (arrows in **b**). The displacement of bone fragments leftward indicates the direction of the bullet path. There are retropulsed fragments within the spinal canal. The bilateral hemothoraces resulted from aortic transection, which was not evident at CT. The aorta is collapsed and not visualized. **(c)** Surface-rendered image of CT data shows the entry wound lateral to the right nipple (arrow). **(d)** Correlative photograph at autopsy shows the entrance wound. **(e)** Photograph at autopsy shows bone fragments protruding from the midthoracic spine (arrows), angled in the direction of the path of the bullet.



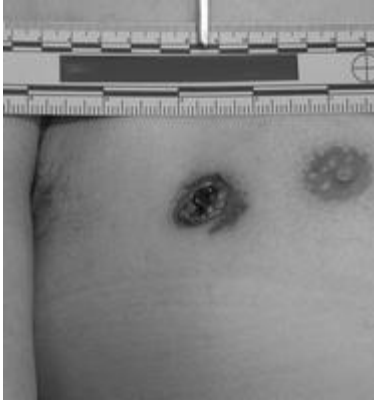
**View larger version (143K):**

[\[in this window\]](#)

[\[in a new window\]](#)

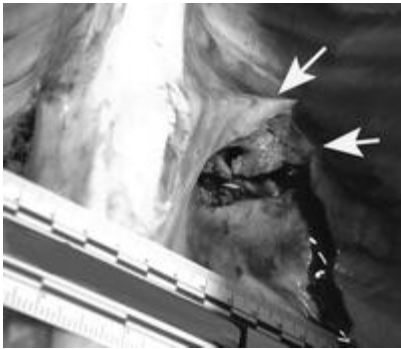
[\[Download PPT slide\]](#)

**Figure 1c:** Lethal gunshot wound to the chest. **(a, b)** Transverse nonenhanced CT image shows the entry wound as an irregular linear soft-tissue defect in the right anterior chest (arrow in **a**) with associated subcutaneous gas. The bullet passed from right to left through the midthoracic vertebral bodies. Bone fragments are present to the left of the vertebral body (arrows in **b**). The displacement of bone fragments leftward indicates the direction of the bullet path. There are retropulsed fragments within the spinal canal. The bilateral hemothoraces resulted from aortic transection, which was not evident at CT. The aorta is collapsed and not visualized. **(c)** Surface-rendered image of CT data shows the entry wound lateral to the right nipple (arrow). **(d)** Correlative photograph at autopsy shows the entrance wound. **(e)** Photograph at autopsy shows bone fragments protruding from the midthoracic spine (arrows), angled in the direction of the path of the bullet.



**View larger version**  
(143K):  
[\[in this window\]](#)  
[\[in a new window\]](#)  
[\[Download PPT slide\]](#)

**Figure 1d:** Lethal gunshot wound to the chest. **(a, b)** Transverse nonenhanced CT image shows the entry wound as an irregular linear soft-tissue defect in the right anterior chest (arrow in **a**) with associated subcutaneous gas. The bullet passed from right to left through the midthoracic vertebral bodies. Bone fragments are present to the left of the vertebral body (arrows in **b**). The displacement of bone fragments leftward indicates the direction of the bullet path. There are retropulsed fragments within the spinal canal. The bilateral hemothoraces resulted from aortic transection, which was not evident at CT. The aorta is collapsed and not visualized. **(c)** Surface-rendered image of CT data shows the entry wound lateral to the right nipple (arrow). **(d)** Correlative photograph at autopsy shows the entrance wound. **(e)** Photograph at autopsy shows bone fragments protruding from the midthoracic spine (arrows), angled in the direction of the path of the bullet.



**View larger version** (149K):  
[\[in this window\]](#)  
[\[in a new window\]](#)  
[\[Download PPT slide\]](#)

**Figure 1e:** Lethal gunshot wound to the chest. **(a, b)** Transverse nonenhanced CT image shows the entry wound as an irregular linear soft-tissue defect in the right anterior chest (arrow in **a**) with associated subcutaneous gas. The bullet passed from right to left through the midthoracic vertebral bodies. Bone fragments are present to the left of the vertebral body (arrows in **b**). The displacement of bone fragments leftward indicates the direction of the bullet path. There are retropulsed fragments within the spinal canal. The bilateral hemothoraces resulted from aortic transection, which was not evident at CT. The aorta is collapsed and not visualized. **(c)** Surface-rendered image of CT data shows the entry wound lateral to the right nipple (arrow). **(d)** Correlative photograph at autopsy shows the entrance wound. **(e)** Photograph at autopsy shows bone fragments protruding from the midthoracic spine (arrows), angled in the direction of the path of the bullet.

### **Gunshot Wound Track Features and Specific Organ Injury**

*Head and neck.*—Gunshot wounds in the head and neck were identified by the presence of gas and metallic fragments along the bullet paths that connected to entry and exit defects that were present along the skin surface. When the bullet passed through bone, bone spicules were embedded in the bullet path. Although gas, bone, and metal were present in the brain parenchyma in those subjects with tracks through the brain, the specific track could not be identified ([Fig 2](#)). In eight of 10 subjects with gunshot wounds through the brain, the brain was



settled in the dependent portion, and pneumocephalus was present in the nondependent portion of the calvarium (Fig 2). There was no evidence of high-attenuation hemorrhage in any of the cases. The brain in the remaining two subjects was extruded from the calvarium. Injury to the vessels in the neck was not identified in any cases by using multidetector CT, and autopsy did not reveal injury to major neck vessels.



**View larger version**  
(93K):

[\[in this window\]](#)

[\[in a new window\]](#)

[\[Download PPT slide\]](#)

**Figure 2a:** Features of a gunshot wound to the head at virtual autopsy. (a, b) Transverse CT images of a lethal gunshot wound to the head show multiple calvarial fractures, posterior settling of the brain, and pneumocephalus. Metallic fragments and foci of gas are present in the left cerebellum in b. A distinct linear bullet track is not present. (c) Three-dimensional volume-rendered image of the skull shows the comminuted fracture of the posterior skull.



**View larger version**  
(104K):

[\[in this window\]](#)

[\[in a new window\]](#)

[\[Download PPT slide\]](#)

**Figure 2b:** Features of a gunshot wound to the head at virtual autopsy. (a, b) Transverse CT images of a lethal gunshot wound to the head show multiple calvarial fractures, posterior settling of the brain, and pneumocephalus. Metallic fragments and foci of gas are present in the left cerebellum in b. A distinct linear bullet track is not present. (c) Three-dimensional volume-rendered image of the skull shows the comminuted fracture of the posterior skull.



**View larger version**

(117K):

[\[in this window\]](#)

[\[in a new window\]](#)

[\[Download PPT slide\]](#)

**Figure 2c:** Features of a gunshot wound to the head at virtual autopsy. **(a, b)** Transverse CT images of a lethal gunshot wound to the head show multiple calvarial fractures, posterior settling of the brain, and pneumocephalus. Metallic fragments and foci of gas are present in the left cerebellum in **b**. A distinct linear bullet track is not present. **(c)** Three-dimensional volume-rendered image of the skull shows the comminuted fracture of the posterior skull.

*Chest.*—Gunshot tracks in the lungs were present in nine subjects. Six subjects had bilateral lung tracks, and three had unilateral tracks. All lung tracks were associated with an ipsilateral hemopneumothorax of variable size. All tracks (100%) were characterized by a linear path of gas containing small metallic and bone fragments surrounded by higher-attenuation hemorrhage and multiple cystic spaces that varied in diameter from 1–2 mm to 1.5–2.0 cm ([Figs 3, 4](#)). Five subjects had injury to major vascular structures within the chest. CT aided in identification of major vascular or cardiac injury in only one (20%) of the five subjects with major vascular injury. This single subject had a gunshot wound track through the heart. In the remaining four cases, vascular injury was suspected on the basis of the presence of mediastinal hemorrhage, large hemothoraces ([Fig 1](#)), or hemopneumopericardium ([Fig 4c](#)), but the injured vascular structures (right atrium and aorta, main pulmonary artery, aortic arch, and right pulmonary vein) could not be identified, even after the final autopsy findings were revealed.

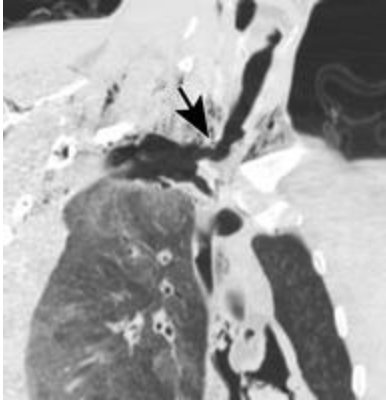


**Figure 3a:** Features of a pulmonary gunshot wound track shown at virtual autopsy. **(a)** Oblique CT image of the neck and chest shows a gunshot wound path through the trachea (arrow) and right lung apex. **(b)** Transverse CT image of the upper chest shows a linear high-attenuation wound track (arrow) containing numerous small cystic spaces (arrowhead). Autopsy showed a hemorrhagic defect at the site of bullet penetration of the trachea (not shown).

**View larger version (159K):**

[\[in this window\]](#)

[\[in a new window\]](#)

[\[Download PPT slide\]](#)

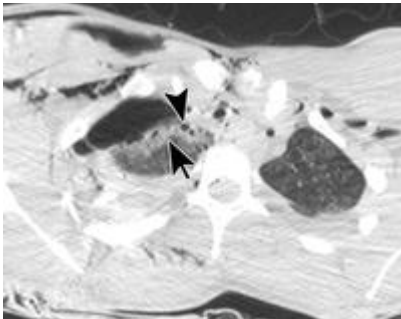


**Figure 3b:** Features of a pulmonary gunshot wound track shown at virtual autopsy. **(a)** Oblique CT image of the neck and chest shows a gunshot wound path through the trachea (arrow) and right lung apex. **(b)** Transverse CT image of the upper chest shows a linear high-attenuation wound track (arrow) containing numerous small cystic spaces (arrowhead). Autopsy showed a hemorrhagic defect at the site of bullet penetration of the trachea (not shown).

**View larger version (127K):**

[\[in this window\]](#)

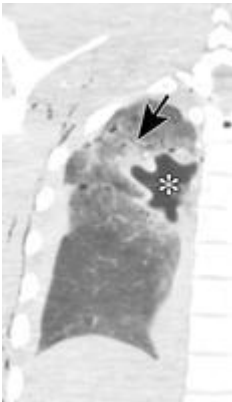
[\[in a new window\]](#)

[\[Download PPT slide\]](#)



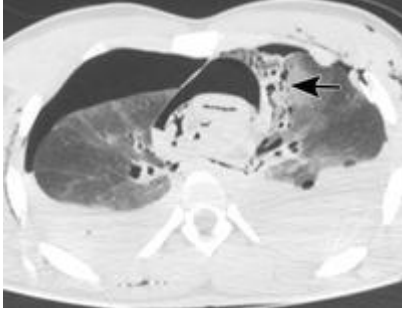
**View larger version**  
(171K):  
[\[in this window\]](#)  
[\[in a new window\]](#)  
[\[Download PPT slide\]](#)

**Figure 4a:** Lethal gunshot wound to the chest. Bullet entered through the right shoulder and passed through the right scapula, right lung apex, pulmonary trunk, pericardium, and lingula. **(a)** Volume-rendered image of CT data shows the bullet path through the scapula (arrow). **(b)** Coronal CT image shows the bullet path (arrow) through the right apex with a large cavity (\*). **(c)** Transverse CT image shows a hemopneumopericardium, collapsed heart, multiple cystic spaces (arrow) in the lingula along the bullet track, bilateral hemopneumothorax, and subcutaneous gas.



**View larger version**  
(73K):  
[\[in this window\]](#)  
[\[in a new window\]](#)  
[\[Download PPT slide\]](#)

**Figure 4b:** Lethal gunshot wound to the chest. Bullet entered through the right shoulder and passed through the right scapula, right lung apex, pulmonary trunk, pericardium, and lingula. **(a)** Volume-rendered image of CT data shows the bullet path through the scapula (arrow). **(b)** Coronal CT image shows the bullet path (arrow) through the right apex with a large cavity (\*). **(c)** Transverse CT image shows a hemopneumopericardium, collapsed heart, multiple cystic spaces (arrow) in the lingula along the bullet track, bilateral hemopneumothorax, and subcutaneous gas.



**View larger version (106K):**

[\[in this window\]](#)

[\[in a new window\]](#)

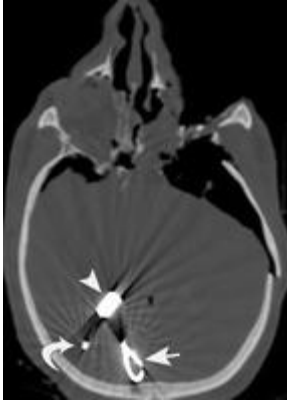
[\[Download PPT slide\]](#)

**Figure 4c:** Lethal gunshot wound to the chest. Bullet entered through the right shoulder and passed through the right scapula, right lung apex, pulmonary trunk, pericardium, and lingula. **(a)** Volume-rendered image of CT data shows the bullet path through the scapula (arrow). **(b)** Coronal CT image shows the bullet path (arrow) through the right apex with a large cavity (\*). **(c)** Transverse CT image shows a hemopneumopericardium, collapsed heart, multiple cystic spaces (arrow) in the lingula along the bullet track, bilateral hemopneumothorax, and subcutaneous gas.

*Abdomen.*—Three gunshot wound tracks through the abdomen were identified in our subjects in addition to one gunshot wound track of the chest that terminated in the left upper quadrant. The tracks through the abdomen were associated with collections of gas and metal along the bullet path. Perforation of the colon was present in one patient. The site of perforation could not be identified at CT but was suspected prior to autopsy because a portion of the colon was herniated through the abdominal wall, and there was hemorrhage within the mesentery. In one subject, the bullet path tracked through the liver, which was evident by the pattern of gas through the liver. However, there was no evidence of altered hepatic attenuation to estimate the degree of hemorrhage or tissue damage along the track.

### **Metallic Fragment Analysis**

In all cases, metallic fragment localization was precise. At autopsy, jackets, lead core fragments, and penetrators were removed at the discretion of the pathologist. Fragments were recovered in nine cases. All removed fragments were identified at CT prior to knowledge of the autopsy results. The lead core of the bullet and fragments of the lead were evident as high-attenuation material of variable sizes and shapes. The bullet jacket is also of high attenuation but had a more irregular shape and was larger compared with the lead core ([Fig 4](#)). In two cases, the penetrator was present and was identified as a rectangular well-defined fragment ([Fig 5](#)).



**View larger version**  
(77K):

[\[in this window\]](#)

[\[in a new window\]](#)

[\[Download PPT slide\]](#)

**Figure 5:** Lethal gunshot wound to the orbit and head. Transverse CT image shows three distinct metallic fragments in the brain parenchyma that correlate to the jacket (straight arrow), penetrator (arrowhead), and a fragment of the lead core (curved arrow). There are multiple calvarial fractures, pneumocephalus, and destruction of the left orbit.

[▲TOP](#)  
[▲ABSTRACT](#)  
[▲INTRODUCTION](#)  
[▲MATERIALS AND METHODS](#)  
[▲RESULTS](#)  
[▪DISCUSSION](#)  
[▼ADVANCES IN KNOWLEDGE](#)  
[▼References](#)

## ► DISCUSSION

The use of CT for postmortem imaging was reported in the medical literature more than 10 years ago (7,8). However, it was not until the past few years that the use of multidetector CT as a virtual autopsy technique was described (9). State-of-the-art multidetector CT scanners are optimal for virtual autopsy because volume acquisition of isotropic data sets may be interpreted in two- and three-dimensional planes that closely replicate conventional autopsy.

Although results were obtained from a small series of subjects in our study, they show that virtual autopsy can reliably aid identification of the site of lethal injury and correct prediction of the majority of gunshot wound tracks in gunshot wound victims. Eighty-seven percent of gunshot wound paths were correctly predicted in our study group. We encountered two limitations to the identification of the correct gunshot wound path: intersecting paths and paths through extremities not included in the field of view of the scan. Comingling or crossing paths in subjects who have sustained multiple gunshot wounds made interpretation of the correct path impossible at CT. Comingling bullet paths may be difficult for the forensic pathologists to confidently identify at

conventional autopsy. In one of our subjects, accurate prediction of the paths of multiple gunshot wounds at the autopsy could not be achieved. In contrast, single gunshot wound paths can be predicted on the basis of applying traditional radiographic methods: directionality of bone and metal fragments and beveling of bone in the direction of the path (5). Rigor mortis affected the positioning of several patients and contributed to the five gunshot wound paths that were missed in the elbow region.

Results of our study indicate that the CT features of gunshot wound tracks are typically linear tissue defects that contain gas and metallic fragments. If the bullet passes through bone as in an intermediate target, bone fragments also are present along the track. In the lungs, the finding of hemorrhage in and around the track was uniformly accentuated by residual aerated lung. Cystic spaces were present along all tracks in the lung. The cysts may represent cavities caused by bullet tumbling, residual temporary cavities formed by the kinetic energy of the bullet, or tissue injury from secondary or intermediate projectiles. Gunshot wounds through the brain were characterized by foci of gas, metallic fragments, and bone. However, a distinct linear track within the brain could not be identified in any of the cases. Evidence of intracranial hemorrhage also was not present. Because our subjects were scanned an average of 3.5 days after death, the most likely explanation for the absence of a discrete track through brain parenchyma and high-attenuation acute hemorrhage is decomposition of the brain and subsequent breakdown of blood products.

Fragment analysis and the pattern of fragment deposition along the gunshot wound track is excellently depicted on two-dimensional multiplanar images, as well as on three-dimensional images, that have thresholds adjusted for metal attenuation. We have shown that the characteristic appearances of the bullet jacket and lead core can be differentiated at CT. Further study is necessary to refine the identification of metal fragments on the basis of metal composition at CT. Once refined, virtual autopsy has the potential of aiding in the identification of metal fragments according to their composition, which would accurately guide forensic pathologists to the site of the most important metal fragments.

The major limitation of our study was the presence of decompositional changes that may have affected our CT interpretation and the detection of discrete gunshot wound tracks through the brain and the CT features of acute hemorrhage. In addition, our study population consisted of victims who sustained multiple gunshot wounds, making interpretation of gunshot wound tracks more difficult. We had the advantage, however, of being able to review autopsy reports and photographs to validate our findings. Fragment analysis was limited because only dominant fragments and those related to the lethal injury were removed. Finally, our small study population limits the conclusions that can be drawn from the study. Statistical tests were not performed as a consequence of the small study size, and, therefore, our results need to be confirmed in a larger series of subjects with sufficient numbers for statistical analysis.

In conclusion, we have shown that virtual autopsy with multidetector CT can aid prediction of lethal wound and fragment localization in victims with high-velocity gunshot wounds. Single-gunshot-wound tracks are well defined. The major limitation occurs in classifying and identifying intersecting and comingling tracks.

<a href="#">▲TOP</a>
<a href="#">▲ABSTRACT</a>
<a href="#">▲INTRODUCTION</a>
<a href="#">▲MATERIALS AND METHODS</a>
<a href="#">▲RESULTS</a>
<a href="#">▲DISCUSSION</a>
▪ <a href="#">ADVANCES IN KNOWLEDGE</a>
▼ <a href="#">References</a>

## ▶ **ADVANCES IN KNOWLEDGE**

- Virtual autopsy with multidetector CT can be used for the prediction of the site of lethal injury and the extent of organ injury in subjects who have died from high-velocity gunshot wounds.
- Virtual autopsy with multidetector CT is useful for characterization of wound tracks and location of metallic fragments from high-velocity gunshot wounds.

## ▶ **FOOTNOTES**

Authors stated no financial relationship to disclose.

The opinions and assertions contained herein are the private views of the authors and are not to be construed as official or as reflecting the view of the Departments of the Army, Navy, Air Force, or Defense.

**Author contributions:** Guarantors of integrity of entire study, A.D.L., C.T.M.; study concepts/study design or data acquisition or data analysis/interpretation, all authors; manuscript drafting or manuscript revision for important intellectual content, all authors; manuscript final version approval, all authors; literature research, A.D.L.; clinical studies, R.M.A., C.T.M., J.M.G., H.T.H., H.R.C.; experimental studies, C.T.M., J.M.G.; statistical analysis, R.M.A., H.T.H., L.P.; and manuscript editing, A.D.L., R.M.A., C.T.M., H.T.H., H.R.C., L.P.

## ▶ **References**



<a href="#">▲TOP</a>
<a href="#">▲ABSTRACT</a>
<a href="#">▲INTRODUCTION</a>
<a href="#">▲MATERIALS AND METHODS</a>
<a href="#">▲RESULTS</a>
<a href="#">▲DISCUSSION</a>
<a href="#">▲ADVANCES IN KNOWLEDGE</a>
• References

1. Brogdon BG. Forensic radiology. Boca Raton, Fla: CRC, 1998.
2. Fatteh AV, Mann GT. The role of radiology in forensic pathology. Med Sci Law 1969;9:27–30.[\[Medline\]](#)
3. Mann GT, Fatteh AB. The role of radiology in the identification of human remains: report of a case. J Forensic Sci Soc 1968;8:67–68.[\[Medline\]](#)
4. Thali MJ, Yen K, Schweitzer W, et al. Virtopsy, a new imaging horizon in forensic pathology: virtual autopsy by postmortem multislice computed tomography (MSCT) and magnetic resonance imaging (MRI)—a feasibility study. J Forensic Sci 2003;48:386–403.[\[Medline\]](#)
5. Di Maio VJM. Gunshot wounds: practical aspects of firearms, ballistics, and forensic techniques. Boca Raton, Fla: CRC, 1999.
6. Thali MJ, Yen K, Vock P, et al. Image-guided virtual autopsy findings of gunshot victims performed with multi-slice computed tomography and magnetic resonance imaging and subsequent correlation between radiology and autopsy findings. Forensic Sci Int 2003;138:8–16.[\[CrossRef\]](#)[\[Medline\]](#)
7. Donchin Y, Rivkind AI, Bar-Ziv J, Hiss J, Almog J, Drescher M. Utility of postmortem computed tomography in trauma victims. J Trauma 1994;37:552–555.[\[Medline\]](#)
8. Wallace SK, Cohen WA, Stern EJ, Reay DT. Judicial hanging: postmortem radiographic CT, and MR imaging features with autopsy confirmation. Radiology 1994;193:263–267.[\[Abstract/Free Full Text\]](#)
9. Thali MJ, Schweitzer W, Yen K, et al. New horizons in forensic radiology: the 60-second digital autopsy—full-body examination of a gunshot victim by multislice computed tomography. Am J Forensic Med Pathol 2003;24:22–27.[\[CrossRef\]](#)[\[Medline\]](#)

**This article has been cited by other articles:**



H. T. Harcke, A. D. Levy, J. M. Getz, and S. R. Robinson

**MDCT Analysis of Projectile Injury in Forensic Investigation**

Am. J. Roentgenol., February 1, 2008; 190(2): W106 - W111.

[\[Abstract\]](#) [\[Full Text\]](#) [\[PDF\]](#)

*This Article*

- ▶ [Abstract](#) **FREE**
- ▶ [Figures Only](#)
- ▶ [Full Text \(PDF\)](#)
- ▶ **All Versions of this Article:**  
[2402050972v1](#)  
**240/2/522 *most recent***
- ▶ [Submit a response](#)
- ▶ [Alert me when this article is cited](#)
- ▶ [Alert me when eLetters are posted](#)
- ▶ [Alert me if a correction is posted](#)

*Services*

- ▶ [Email this article to a friend](#)
- ▶ [Similar articles in this journal](#)
- ▶ [Similar articles in PubMed](#)
- ▶ [Alert me to new issues of the journal](#)
- ▶ [Download to citation manager](#)
- ▶ [© Get Permissions](#)

*Citing Articles*

- ▶ [Citing Articles via HighWire](#)
- ▶ [Citing Articles via Google Scholar](#)

*Google Scholar*

- ▶ [Articles by Levy, A. D.](#)
- ▶ [Articles by Pearse, L. A.](#)
- ▶ [Search for Related Content](#)

*PubMed*

- ▶ [PubMed Citation](#)
- ▶ [Articles by Levy, A. D.](#)
- ▶ [Articles by Pearse, L. A.](#)

 <http://radiology.rsna.org/cgi/content/full/240/2/522>